

Characteristics of Strong Ground Motion Areas by Earthquake Cycle Simulations.

P. Galvez^(1*), P. Somerville⁽²⁾, and A. Pethukin⁽³⁾

(1) AECOM, Switzerland.
*King Abdullah University of Science and Technology (KAUST).

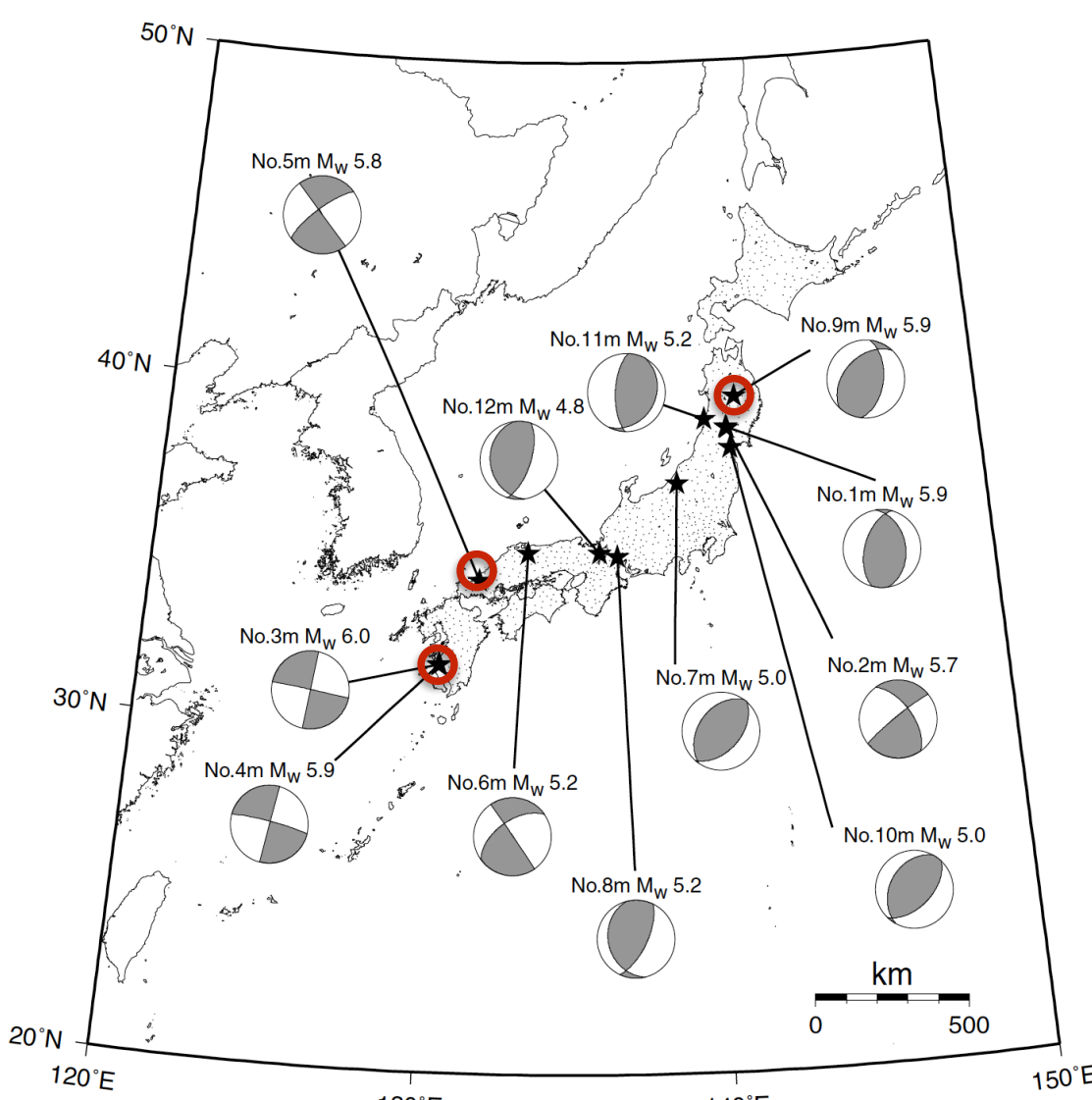
(2). Seismology department, AECOM, USA.

(3). Geo-Research Institute, Japan.

Introduction.

Strong Ground Motion Generation Areas (SMGA's)

(a) Mw < 6.0 crustal earthquakes in Japan



Miyake et al. (2003)

(b) Region of high slip = Slip asperity
Region of high slip velocity = SMGA

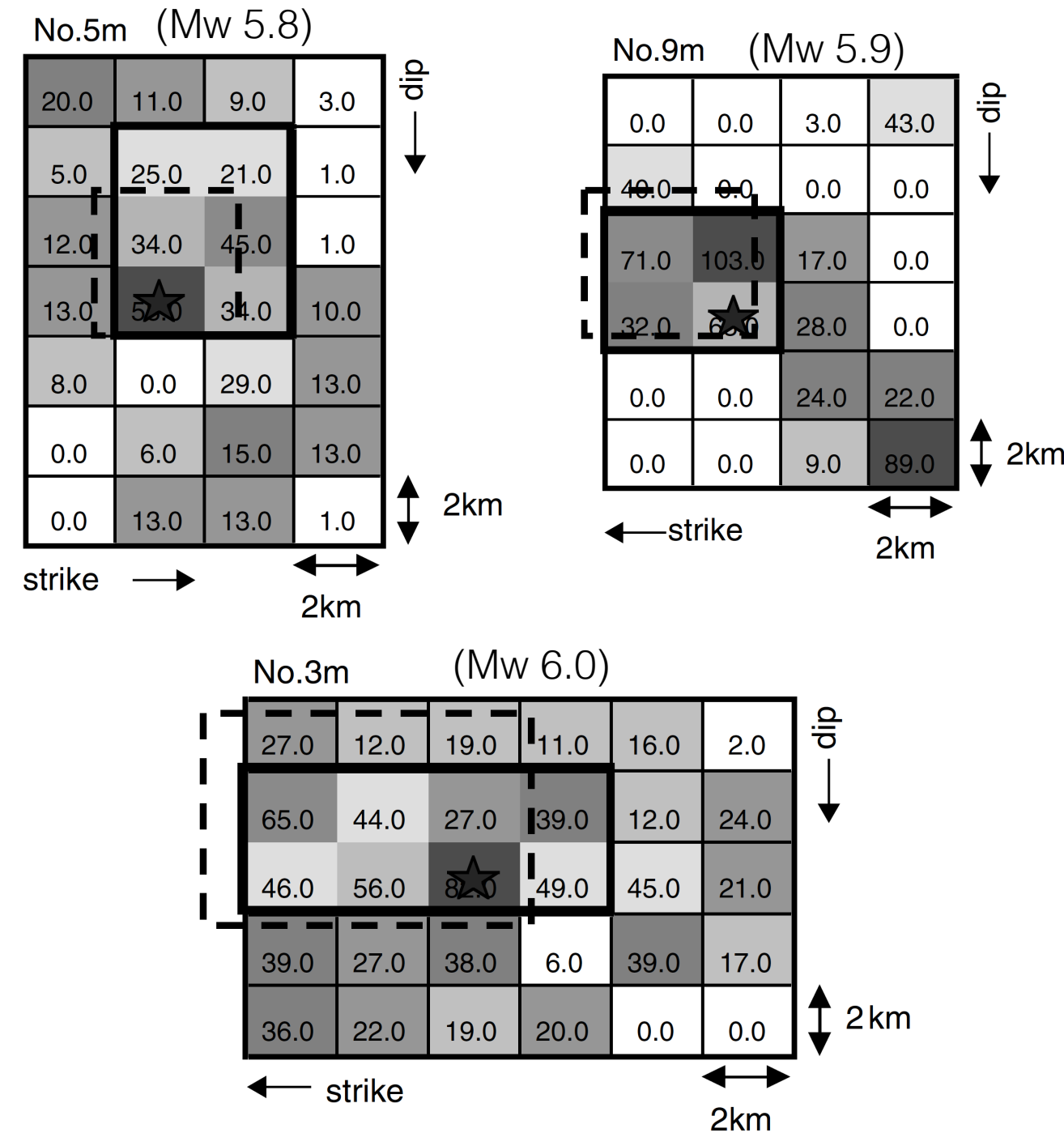


Figure 1. (a) Epicenter location (Solid starts) for 12 crustal earthquakes (Mw 4.8-6.0). (b) Comparison of the strong ground motion generation areas and asperity areas, which are characterized by the heterogeneous slip distributions obtained by waveform inversions of Miyakoshi et al. (2000). From the left to the right, the 1997 Kagoshima ken Hokuseibu earthquake (number 3m), 1997 Yamaguchi-ken Hokubu earthquake (number 5m), and 1998 Iwate-ken Nariku Hokubu earthquake (number 9m). The thick solid lines show the boundaries of the slip asperities according to Somerville et al. (1999). The broken lines show the boundaries of the strong ground motion generation areas. Numbers on each subfault are slip, in centimeters, estimated by waveform inversions. Source: Miyake et al. (2003).

Strong Ground Motion Generation Areas (SMGA's)

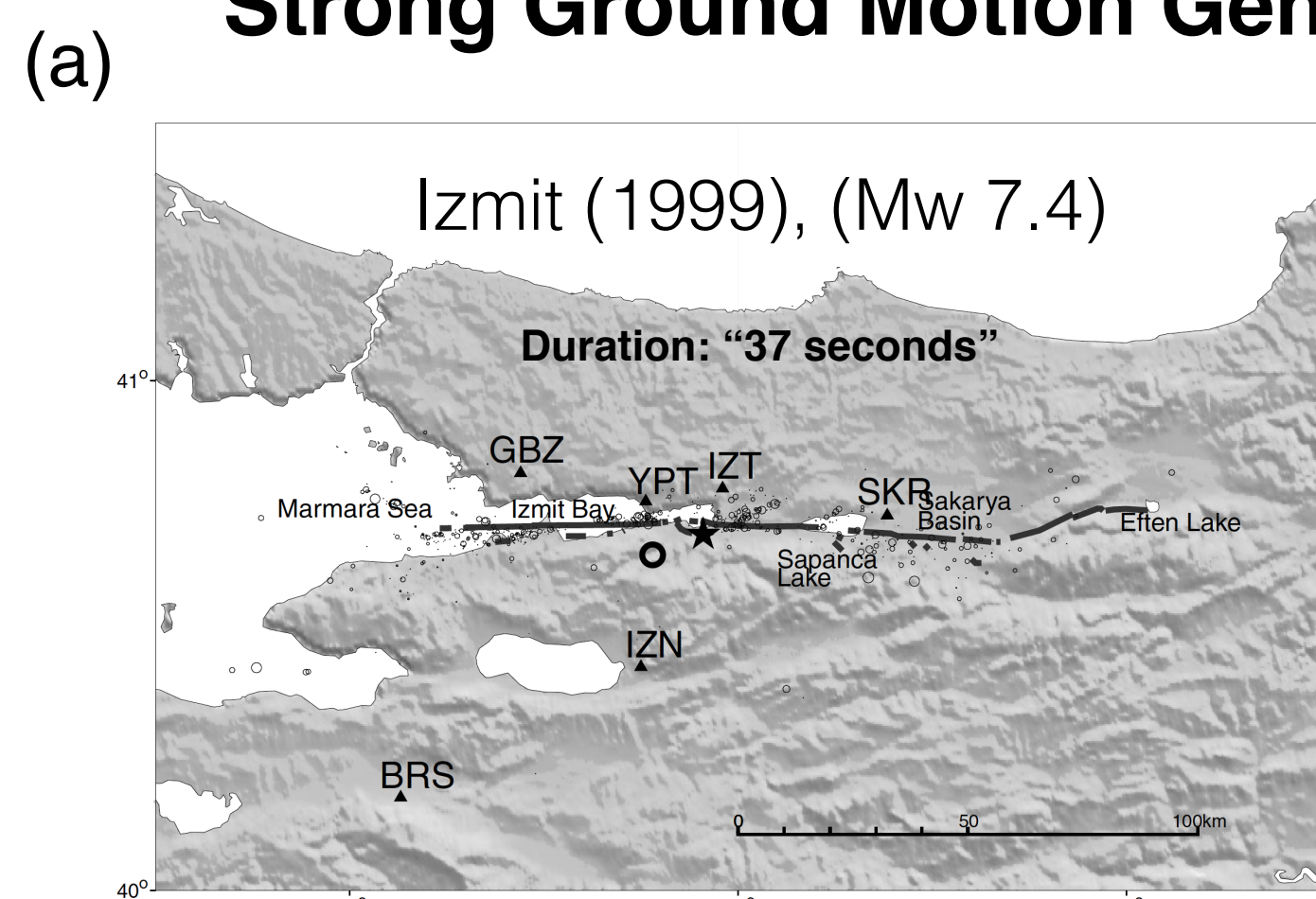
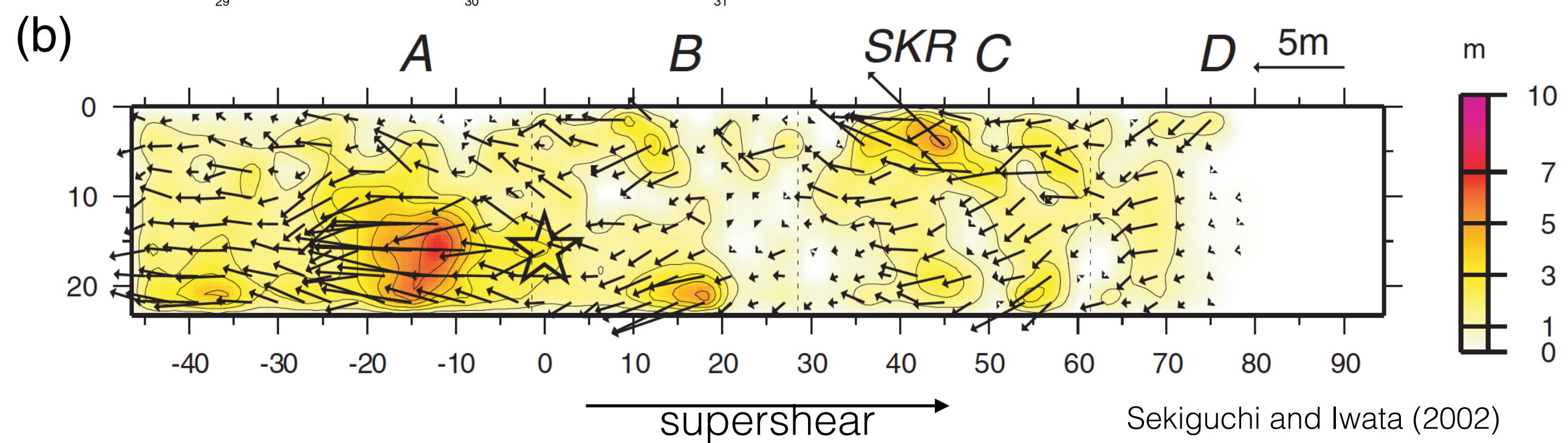


Figure 2. The black solid line represents the surface rupture of the Mw 7.4, 1999 Izmit earthquake. The black start indicates the epicenter and the small dot points the first day aftershock distribution (Honkura et al., 2000; Ito et al., 2002). (b) Final slip distribution of the source inversion made by Sekiguchi and Iwata (2002).



Sekiguchi and Iwata (2002)

Fault settings.

1. Fault settings

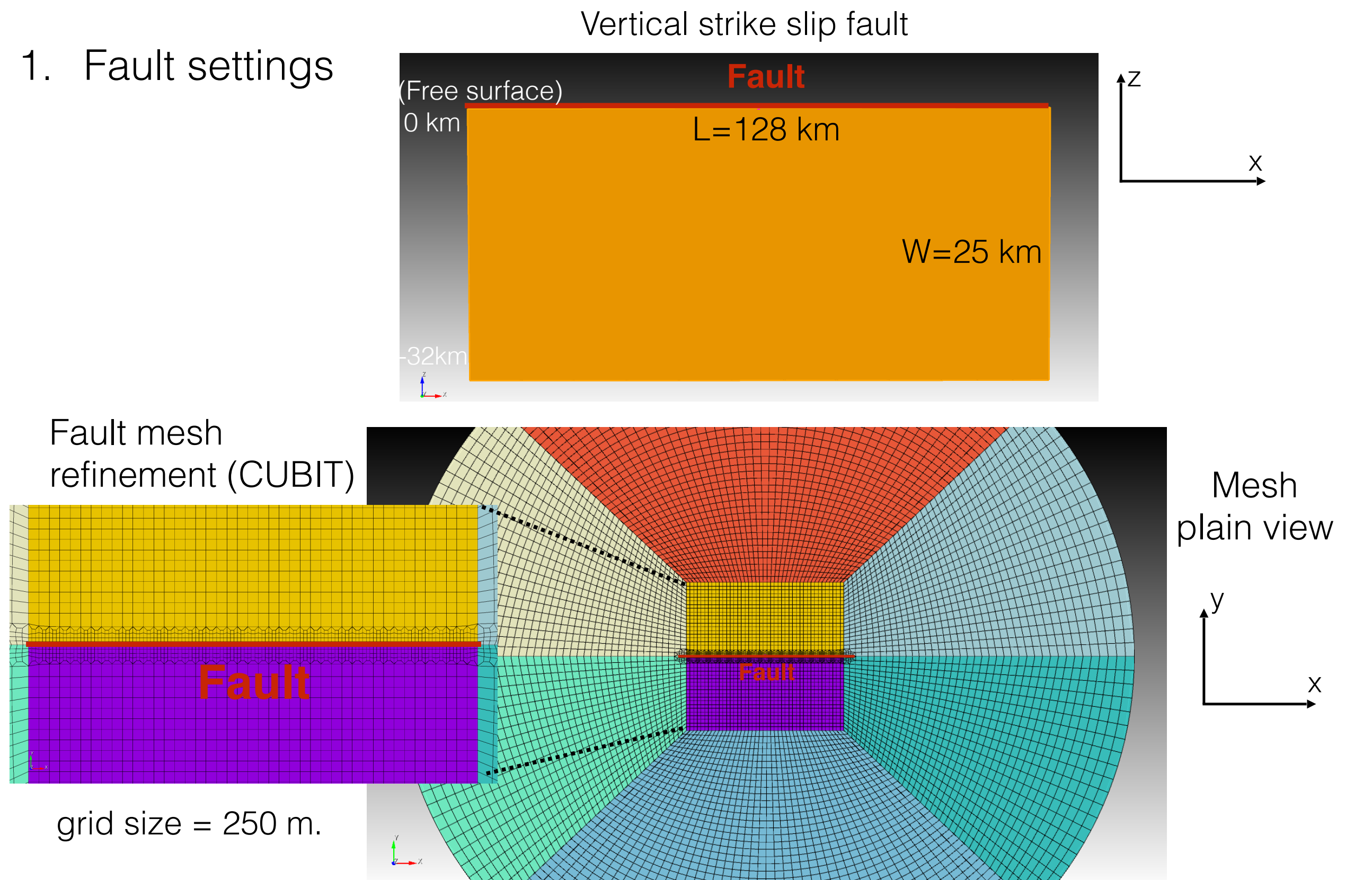


Figure 3. (a) 3D vertical fault with 128 Km length and 32 Km width used for this study. (b) Plain view meshing of the fault domain. We applied strong spherical coarsening where the grid size at the fault plane is 250 meters and increases radially to 5km. We make use of the state-of-the-rate mesher (CUBIT).

(a) Rate and state friction.

$$\frac{\tau}{\sigma} = f^* + a \ln \frac{V}{V^*} + b \ln \frac{V^* \theta}{D_c}$$

$$\dot{\theta} = 1 - \frac{V \theta}{D_c} \quad (\text{Aging Law})$$

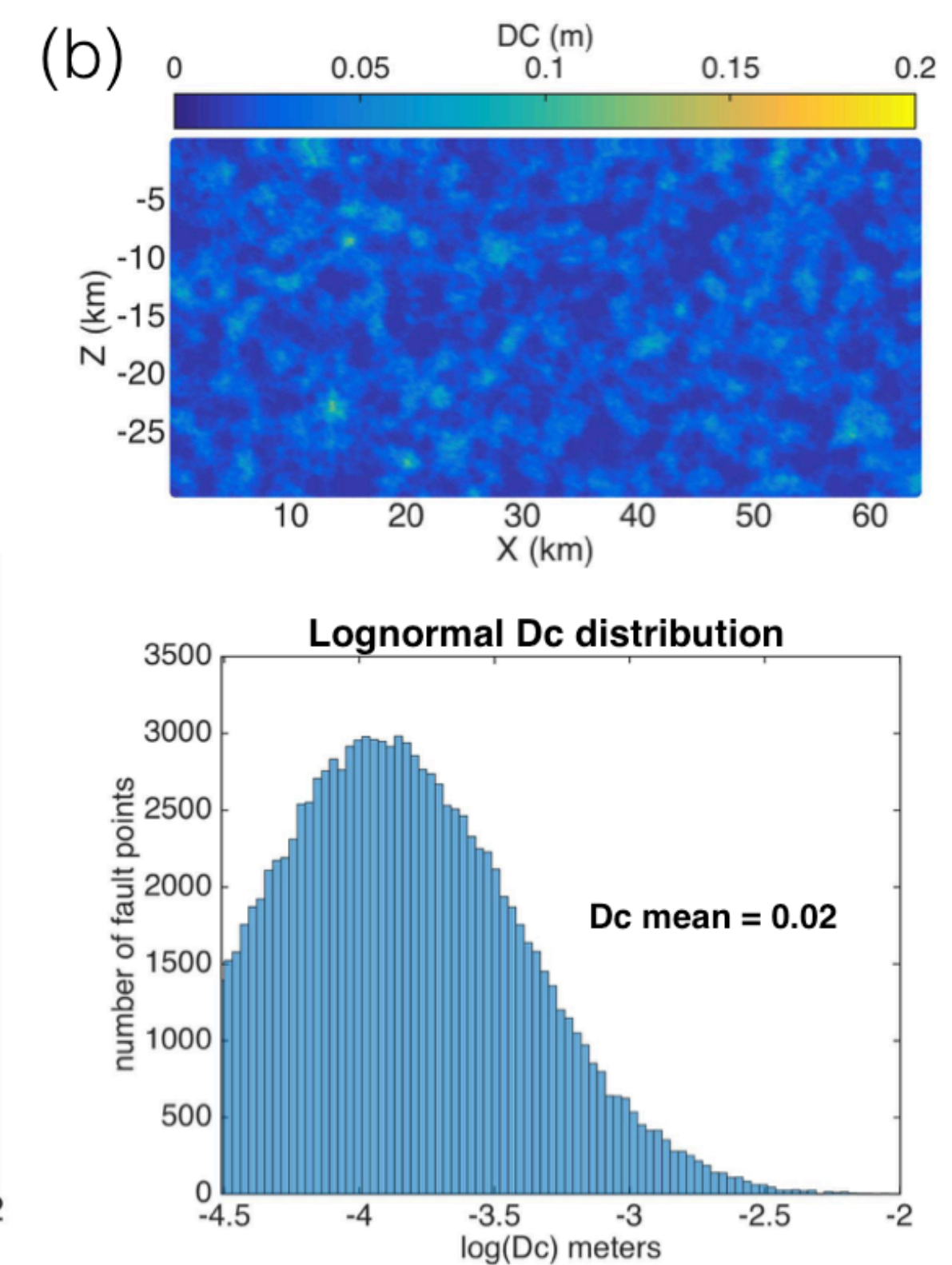
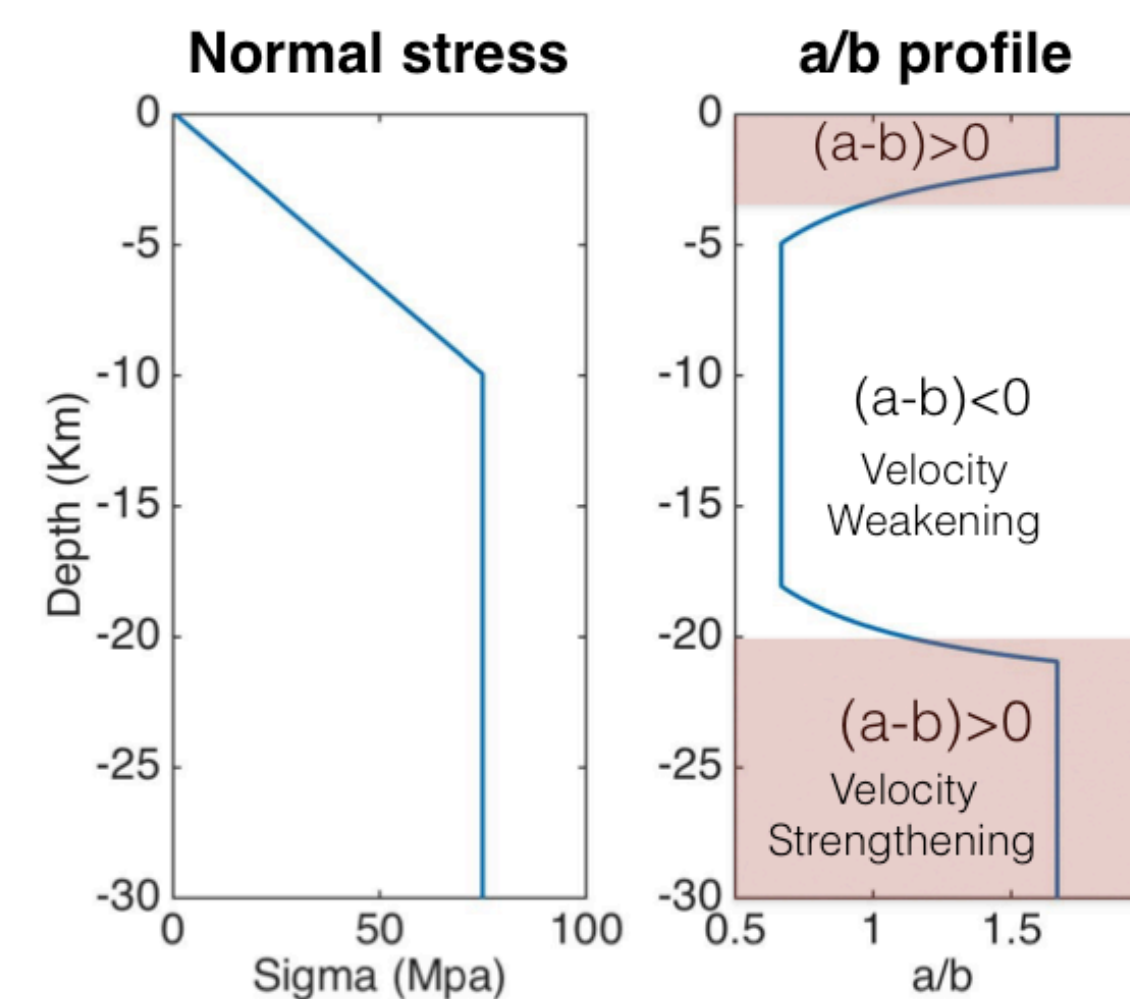


Figure 4. (a) We imposed rate and state friction law in our quasi-dynamic and fully dynamic simulations. The blue solid lines are the normal stress and a/b ratio prescribed on the fault plane. A gradual taper is applied to change the a/b ratio. (b) Critical slip distance (Dc) with a lognormal distribution is prescribed on the fault plane. The Dc mean is 0.02.

Earthquake cycle modeling

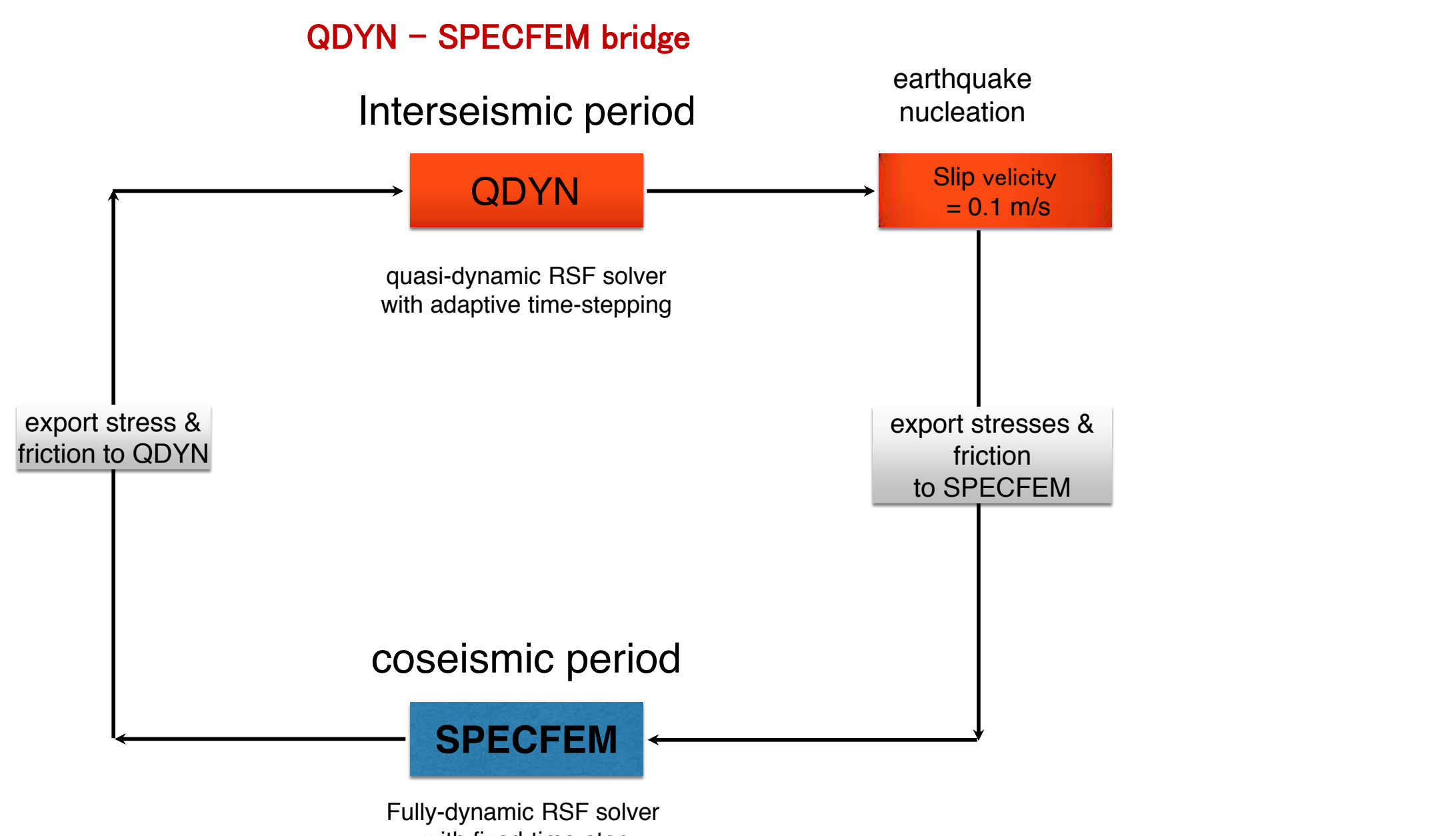


Figure 5. Scheme for the earthquake cycle simulations couple with dynamic rupture used in this study. The interseismic period is resolved with the quasi-dynamic solver QDYN (Luo et al., 2017) with adaptive time stepping and once the slip rate reach 0.1 m/s, the software switch to the fully dynamic solver SPECFEM3D (Galvez et al., 2014) and resolves the rupture process during the coseismic period. Once the rupture ends, friction and stresses are imported back to QDYN to continue with the next earthquake cycle.

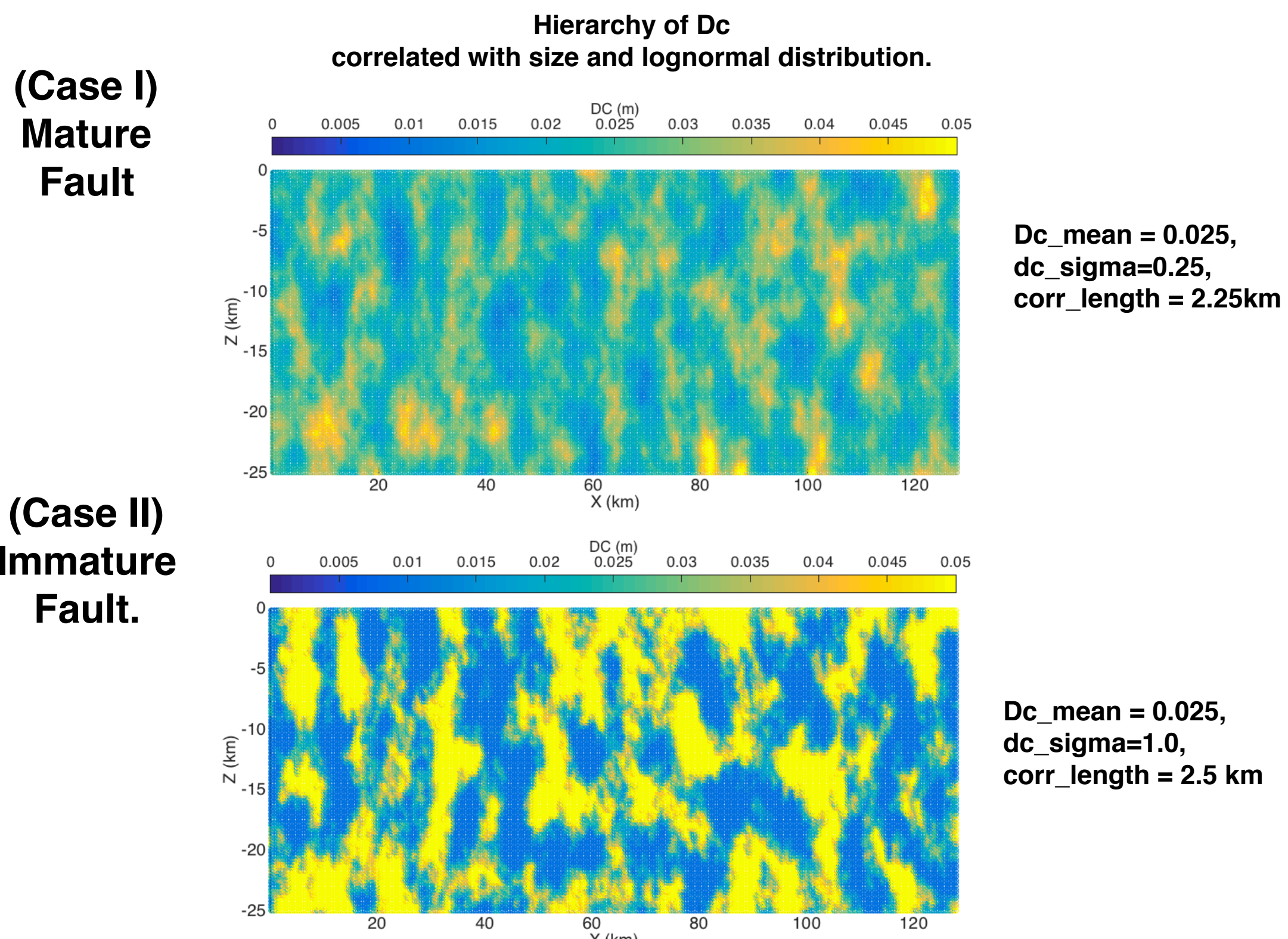


Figure 6. Two fault types have been chosen for this study, where case 1 has lower Dc variability (sigma = 0.25) and represents a mature fault. Case 2 has bigger Dc variability and represents a younger, immature fault. The Dc distribution is adopted from Hillers et al. (2007) and Luo et al. (2017).

Fault rheology and strong ground motion areas

Case I (Mature Fault)

Case II (Immature Fault)

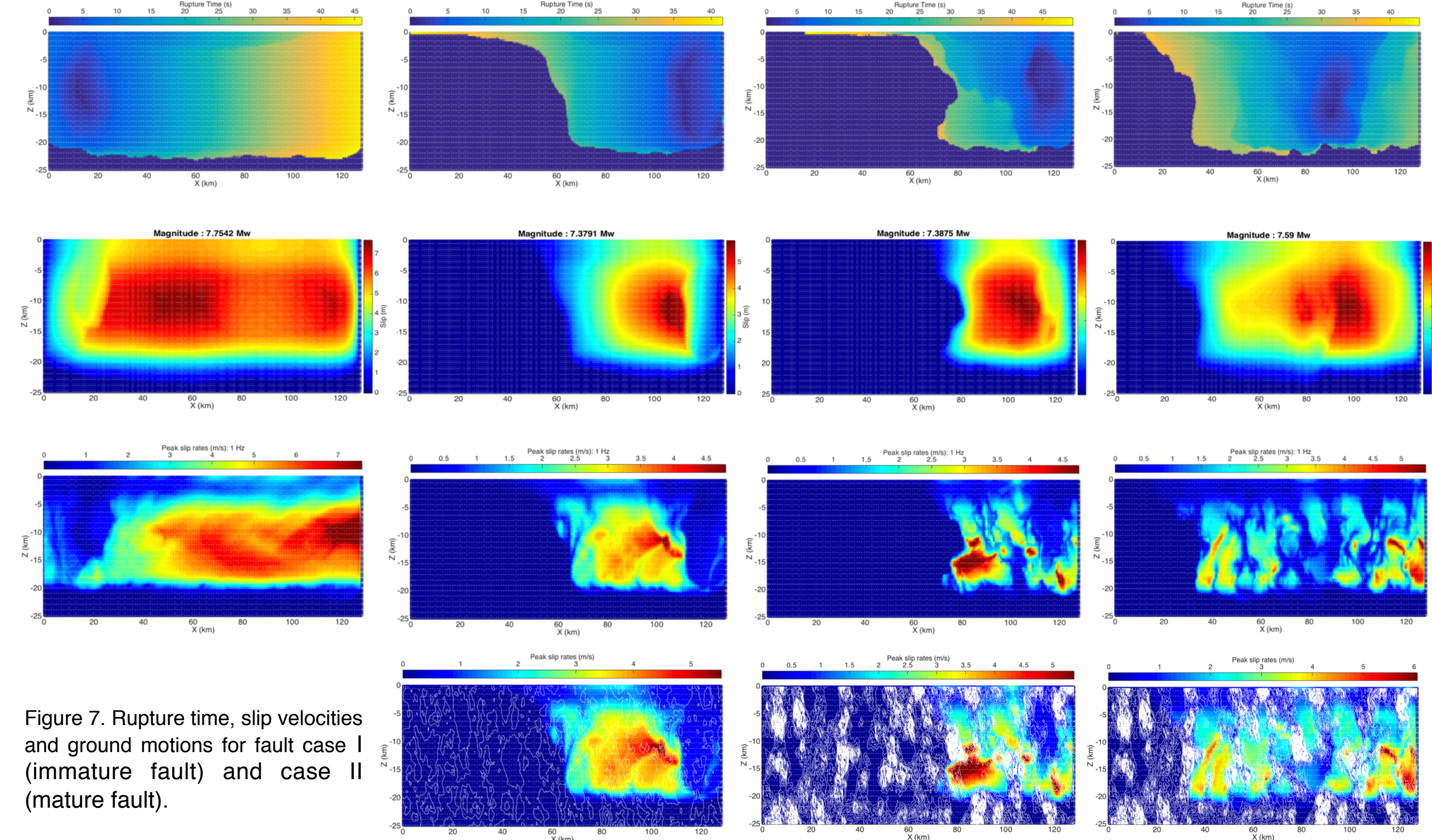
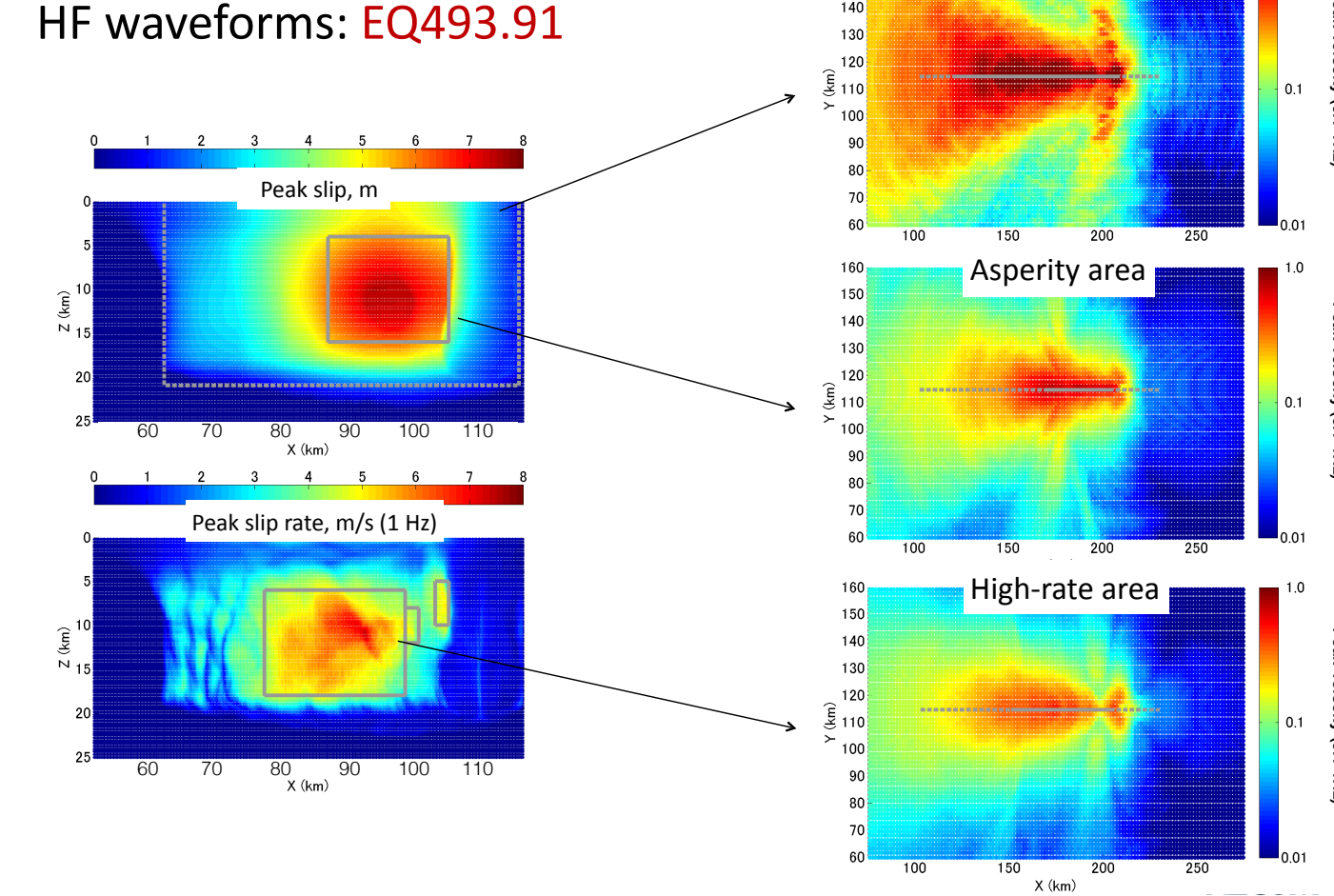
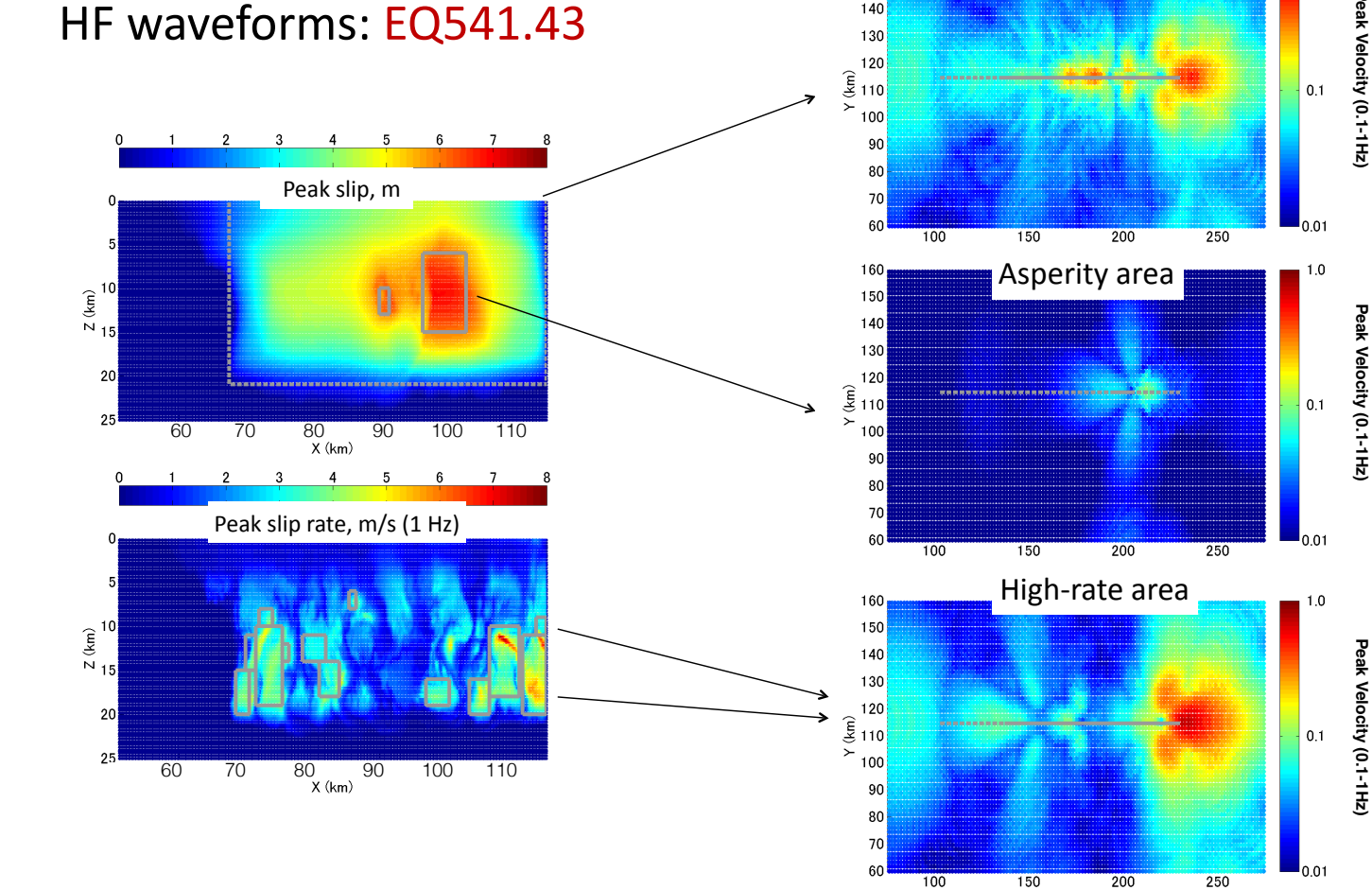


Figure 7. Rupture time, slip velocities and ground motions for fault case I (immature fault) and case II (mature fault).

Comparison of amplitudes of HF waveforms: EQ493.91



Comparison of amplitudes of HF waveforms: EQ541.43



Conclusions.

The correlation between region of high slip (slip asperity) and slip velocities (SMGA's) decreases as the event magnitude increases. For events with Mw > 7.4, slip asperity patches and SMGA's do not seem to overlap at least for immature faults. For very elongated events, the peak slip velocity regions are found at the edges of the fault. However fault segmentation may play a fundamental role in modifying this behavior. Regions of strong ground motions seems to correlate with regions of lower Dc in immature faults. However for mature faults, these correlation seems to disappear.